International Journal of Automotive and Mechanical Engineering (IJAME)
ISSN: 2229-8649 (Print); ISSN: 2180-1606 (Online); Volume 8, pp. 1278-1291, July-December 2013

DOI: http://dx.doi.org/10.15282/ijame.8.2013.17.0105

OVERALL HEAT TRANSFER ENHANCEMENT OF TRIANGULAR OBSTACLES

B. Sahin[1*], E. Manay[1] and V. Ozceyhan[2]

[1]Faculty of Engineering & Architecture, Erzurum Technical University
Erzurum, Turkey
Phone: +90-442-6662528 ; Fax : +90-442-6662535
*Email: bayram.sahin@erzurum.edu.tr
[2]Faculty of Engineering, Erciyes University,
38039 Kayseri, Turkey

ABSTRACT

In this study, the effects of equilateral triangular bodies placed in the channel on heat transfer and pressure drop characteristics were examined numerically. Reynolds number varied from 5000 to 10,000. The effects of the blockage ratio at constant edge length (B=20 mm) and Reynolds number of triangular bodies were investigated. An RNG based k-ε method was used and a constant surface temperature was applied to the bottom wall. The numerical results were presented with respect to temperature contours, local and mean Nusselt number, local and mean surface friction factor changes and heat transfer enhancement ratios. The results showed that the presence of the equilateral obstacles in the flow field enhanced the heat transfer. Temperature distributions behind the bodies were affected by the position of the triangles and the Reynolds number and changed greatly in the vertical direction along the x distance beyond the bluff bodies. The intensity of the oscillations decreased with the increase of the Reynolds number. It was observed that for all cases overall heat transfer enhancement was provided. It was found that the highest values of OHTE were reached at W/B=0 and Re=5.0 and lowest were at W/B=1 and Re=10.0.

***Keywords*:** Triangular body; bluff body; heat transfer enhancement; numerical.

INTRODUCTION

By the use of bluff bodies, not only variation of the flow field, but also heat transfer enhancement is provided. In general, heat transfer enhancement techniques are either passive or active methods. In the basic method, no extra energy is applied from outside to the system upon increasing the heat transfer by the aid of the passive methods. But, the geometrical parameters of the current system are modified in order to increase the heat transfer. The ones frequently used in these processes are extending surfaces, operating the surfaces, replacing the inner elements into the system etc. In active methods, the aim is to enhance heat transfer by giving extra energy like surface vibration, suction or pressing. Due to problems like vibration and acoustic noise as well as the investment and the operating costs, heat transfer enhancement via active methods has not been attracting attention. Research on heat transfer augmentation has been increasing especially in the cooling of electronics and heat recovery systems (Tahseen, Ishak, & Rahman, 2012). In turbulent flows, the aim of the heat transfer enhancement by passive methods is to destroy the viscous sublayer. Inserting inner elements into the channel or pipe flows causes the viscous sublayer to be destroyed (Manay, 2010). The

studies done in this field have shown that several parameters like geometry and geometrical arrangements are also affected on the heat transfer and flow structure. This paper presents a detailed numerical study of the flow around a pair of triangles in a side-by-side arrangement. There are many studies about bluff bodies. Sumner (2010) investigated the flow structures around two identical cylinders in cylinders and presented an overview of the studies including bluff bodies. It was emphasized that flow around would attract attention because of its complexity. Also, much more analysis is required for the transition and evolution between near-wall flow patterns and vortex street modes. Just as the bodies, known as bluff bodies, that are placed into the flow field change the structure of the flow field, they affect the heat transfer in the increasing direction. Srikanth et al. (2010) studied forced convection heat transfer and flow characteristics on a confined triangular prism. An increase in heat transfer from 12.5% to 25% was provided due to the presence of the prism in the flow field. Near a moving wall, heat transfer from a square cylinder was investigated by Dhinakaran (2011). It was found that an existing obstacle in the flow field always increased the heat transfer relative to an isolated one. Heat transfer caused by a bluff body such as a horseshoe vortex generator was examined experimentally by Wang et al. (2012). Heat transfer was enhanced by the use of the horseshoe vortex generator in both single and tandem arrangements.

Dhiman and Hasan (2013) investigated both heat transfer and flow structure around a different flow blockage. A trapezoidal cylinder was used as the bluff body. It was observed that flow separation occurred at values of Reynolds number higher than 5. Steady and unsteady regimes were also analyzed. The limitation was found to be 46–47 for transition from steady to unsteady flow regime. Rosales, Ortega and Humphrey (2001) investigated the flow and heat transfer characteristics around square bluff bodies placed in the channel. The Nusselt number increased and the drag coefficient decreased in the event that the cylinders became closer to the walls. The biggest value of the Strouhal number was obtained when the bodies were at the center of the channel. Abbasi, Turki, and Nasrallah (2001) proposed a model which gave the variation of the Strouhal number with Reynolds number for periodic flow, by examining numerically the heat transfer and the flow characteristics of a heated triangular body. At values of Reynolds number about 45, they observed some passages from symmetrical to periodic form. The highest heat transfer rates were achieved in the case of $Re>45$ relative to that of $Re<45$. Sripattanapipat and Promvonge (2009) placed diamond-shaped obstacles in the channel. At different Reynolds numbers and attack angles of the obstacles, the heat transfer characteristics were investigated under a constant surface temperature condition. It was seen that just as the diamond-shaped elements enhanced heat transfer by about 200–600, the friction losses also increased by 20 to 220 times relative to the smooth channel.

A column consisting of five square elements was left in the flow field at different gap ratios by Chatterjee, Biswas and Amiroudine (2009) and the flow structures and heat transfer were examined. Heat transfer increased in the presence of the square elements. The flow structure and the heat transfer characteristics around plate type bodies at different positions, edge angles, gap ratios and Reynolds numbers were studied by Hanafi, El-Sayed, and Mostafa (2002). Except for the gap ratio of 7 and 10, it was concluded that the flow and heat transfer characteristics were dependent on the plate geometry for all the tested gap ratios. Velayati and Yaghoubi (2005) numerically investigated the efficiency of bluff bodies placed in a uniform flow field as a tandem arrangement. The heat transfer increased with the increase of the Reynolds number and

blockage ratio. Hemida, Spehr, and Krajnovic (2008) numerically studied the flow and local heat transfer around a bundle of cubic elements under constant heat flux and Reynolds number. The heat transfer and the vortex sheddings caused by a cylinder whose surface was heated were investigated by Bhattacharyya and Singh (2010). The variations of Nusselt number and the Richardson number were linear at constant Reynolds number. Another study on heated cylinders was conducted by Bharti, Chabra, and Eswaran. It was concluded that in front of the cylinder the Nusselt number decreased due to the fact that the behavior of the fluid changed from shear weakening towards shear intensifying and took its minimum value at the stagnation point.

Igarashi and Mayumi (2001) studied experimentally the flow and heat transfer phenomena around a rectangle placed as inclined and straight. They determined that the flow is laminar when the inclination is less than 15° or else turbulent. Maximum heat transfer was provided at 0–5°. Juncu (2007) examined the effects of the model parameters on heat transfer in a flow field around two cylinders placed in tandem for different Prandtl numbers at low Reynolds numbers. For different distance ratios of the cylinders in tandem arrangements with equal surface temperatures, Mahir and Altaç (2008) conducted an experimental study in order to investigate the transient forced convection heat transfer. Meinders and Hanjalic (2002) investigated the convection heat transfer of two squares fixed onto the bottom in tandem and in staggered arrangements. In the tandem array, the flow structures are periodic. Nakamura, Igurushi, and Tsutsui (2003) studied the flow and heat transfer parameters around a cube placed at an angle of 45° depending on the cube height at different Reynolds numbers. At the end of the analyses, it was seen that the heat transfer characteristics were different in the case of the tandem arrangement. Based on the results summarized above, one finds that the relationship between Reynolds number and the biasing characteristics of the gap flow depends strongly on the geometry of the bluff body. Because many practical engineering problems are related to the flow field downstream of bluff bodies with different cross-sectional geometries, the present study focused on flow interaction near two triangular bluff bodies in a side-by-side arrangement and was performed for a Reynolds number range varying from 5000 to 10,000 under steady state conditions.

CFD ANALYSIS

Problem Description

In Figure 1, the main features of the test section are shown schematically. The computational domain mainly consists of a two-dimensional channel and dual triangular bodies placed in a side-by-side arrangement. As seen in Figure 1, the channel height (H) of $4B$, and the placement of the bluff bodies (S) was maintained at $x = 8B$, while the channel length was $36B$. To prevent negative pressure effects at the outlet sections, the outlet section was selected to be long enough, and likewise the inlet section was long enough to get a fully developed flow.

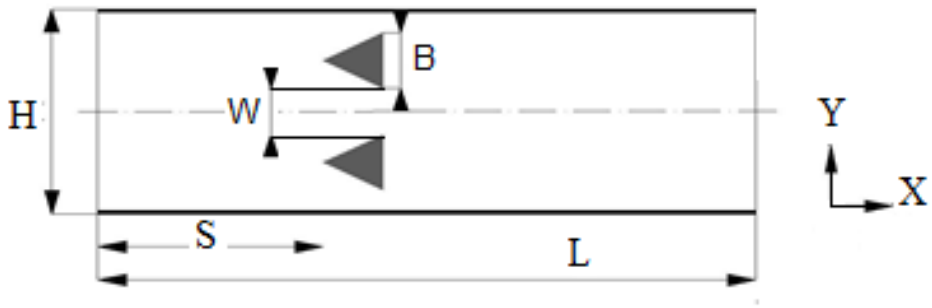

Figure 1. Computational domain and the triangular bodies in side-by-side arrangement.

Numerical Procedure

To determine the velocity and temperature distributions, CFD calculations made with the aid of the computational fluid dynamics (CFD) commercial code of FLUENT version 6.1.22 (2001) are performed, depending on the numerical model, boundary conditions, assumptions, and numerical values. In all the numerical calculations, the segregated manner was selected as the solver type, to take advantage of its ability to prevent convergence problems and oscillations in pressure and velocity fields of strong coupling between the velocity and pressure. The RNG *k-ε* turbulence model is used for simulations and the second order upwind numerical scheme and SIMPLE algorithm, being more stable and economical than other algorithms, are utilized to discretize the governing equations. The converging criteria are taken as 10–6 for the energy and 10−4 for other parameters. In momentum and continuity equations, the thermophysical properties are thought of as constant, and the flow is assumed to be two-dimensional, steady state.

Governing Equations

Continuity conservation:

$$\frac{\partial \rho}{\partial t} + \nabla \cdot \left(\rho \cdot \vec{v} \right) = 0 \tag{1}$$

Momentum conservation:

$$\frac{\partial \left(\rho \cdot \vec{v} \right)}{\partial t} + \nabla \cdot \left(\rho \cdot \vec{v} \cdot \vec{v} \right) = \rho g - \nabla P + \nabla \cdot \left(\vec{\tau} \right) \tag{2}$$

Energy conservation:

$$\frac{\partial \left(\rho E \right)}{\partial t} + \nabla \cdot \left(\vec{v} \cdot \left(\rho E + p \right) \right) = \nabla \cdot \left(k_{eff} \nabla T + \left(\vec{\tau}_{eff} \cdot \vec{v} \right) \right) \tag{3}$$

In Eqs. (2), (3) and (4), ν is the velocity, P is the pressure, T is the temperature, ρ is the density of air. u, v and w are the velocity components in the x, y and z directions

in the Cartesian coordinate system, respectively. The above thermo-physical properties of water are taken as temperature-independent (constant) properties. Because of the fact that the flow is fully turbulent, the turbulent kinetic energy and the dissipation rate of turbulent kinetic energy equations derived from the transport equations are given as below:

$$\frac{\partial}{\partial t}(\rho k)+\frac{\partial}{\partial x_i}(\rho k u_i)=\frac{\partial}{\partial x_j}\left(\alpha_k \mu_{eff}\frac{\partial k}{\partial x_j}\right)+G_k+G_b-\rho\varepsilon-Y_M+S_k \tag{4}$$

$$\frac{\partial}{\partial t}(\rho \varepsilon)+\frac{\partial}{\partial x_i}(\rho \varepsilon u_i)=\frac{\partial}{\partial x_j}\left(\alpha_\varepsilon \mu_{eff}\frac{\partial \varepsilon}{\partial x_j}\right)+C_{1\varepsilon}\frac{\varepsilon}{k}(G_k+C_{3\varepsilon}G_b)-C_{2\varepsilon}\rho\frac{\varepsilon^2}{k}-R_\varepsilon+S_\varepsilon \tag{5}$$

In these equations, G_k represents the generation of turbulence kinetic energy due to the mean velocity gradients, and G_b is the generation of turbulence kinetic energy due to buoyancy. Y_M represents the contribution of the actuating dilatation in compressible turbulence to the overall dissipation rate. The quantities α_k and α_ε are the inverse effective Prandtl numbers for k and ε, respectively. S_k and S_ε are user-defined source

In the RNG *k-ε* turbulence model, the turbulent viscosity is calculated by Eq. (6), terms.

$$d\left(\frac{\rho^2 k}{\sqrt{\varepsilon\mu}}\right)=1.72\frac{\hat{\nu}}{\sqrt{\hat{\nu}^3-1+C_\nu}}d\hat{\nu} \tag{6}$$

where

$$\hat{\nu}=\mu_{eff}/\mu \tag{7}$$

$$C_\nu \approx 100 \tag{8}$$

In high Reynolds numbers, the effective viscosity is calculated via Eq. 9:

$$\mu_t=\rho C_\mu\frac{k^2}{\varepsilon} \tag{9}$$

with C_μ = 0.0845, derived using RNG theory. It is interesting to note that this value of C_μ is very close to the empirically-determined value of 0.09 used in the standard k-ε model (2001). Eq. (10) presented below is used for the calculation of the inverse effective Prandtl numbers, α_k ve α_ε :

$$\left|\frac{\alpha-1.3929}{\alpha_0-1.3929}\right|^{0.6321}\left|\frac{\alpha+2.3929}{\alpha_0+2.3929}\right|^{0.3679}=\frac{\mu_{mol}}{\mu_{eff}} \tag{10}$$

where α_k =1.0. In high Reynolds numbers ($\mu_{mol}/\mu_{eff} \ll 1$), $\alpha_k = \alpha_\varepsilon \approx 1.393$. The main difference between the RNG and standard k-ε models lies in the additional term in the ε equation given by FLUENT 6.1.22 (2001).

$$R = \frac{C_\mu \rho \eta^3 (1 - \eta/\eta_0)}{1 + \beta \eta^3} \frac{\varepsilon^2}{k} \tag{11}$$

$$\eta = S_k / \varepsilon,\ \eta_0 = 4.38 \text{ ve } \beta = 0.012 \tag{12}$$

C1ε, C2ε model constants are obtained analytically by the RNG theory, C1ε=1.42, C2ε=1.68 (FLUENT 6.1.22).

Heat Transfer and Friction Factor

Two parameters of interest for this study are the skin friction coefficient and the Nusselt number. The skin friction coefficient C_f is defined by

$$C_f = \frac{\tau_s}{\frac{1}{2}\rho U_m^2} \tag{13}$$

The heat transfer performance is evaluated by the Nusselt number, which can be obtained by the local temperature gradient as:

$$Nu = -\frac{\partial T}{\partial Z} \tag{14}$$

The average Nusselt number can be calculated as follows:

$$Nu_{av} = \int Nu_x \frac{\partial x}{L} \tag{15}$$

where L is the length of the computational domain. The friction factor is determined from

$$f = \frac{\Delta P}{\frac{1}{2}\rho . U_m{}^2 \frac{L}{H}} \tag{16}$$

in which pressure ΔP is the pressure difference between the channel inlet and exit.

Boundary Conditions

The solution domain of the considered 2D channel flow is geometrically quite simple, which is a rectangle on the x–z plane, enclosed by the inlet, outlet and wall boundaries. The working fluid in all cases is water. The inlet temperature of the water is considered to be uniform at 300 K. On walls, no-slip conditions are used for the momentum equations. A constant surface temperature of 360 K is applied to the bottom wall of the channel. The upper wall is assumed to be adiabatic. Uniform velocity is imposed on the inlet plane and the Reynolds number varies from 5000 to 10,000. The outlet boundary condition is a natural condition which implies zero-gradient conditions at the outlet.

RESULTS AND DISCUSSION

Figures 2, 3 and 4 present the temperature contours for Re=5000 (on the top), Re=7500 (in the middle), Re=10,000 (below) and the legends at the left side. At the bottom side of the channel, the constant surface temperature boundary condition has been applied; as for the top side, it has been adiabatic. At the end of the results obtained, it is seen that the temperature distributions behind the bodies are affected by the position of the triangles and the Reynolds number. Along the x distance beyond the bluff bodies, the temperature variations change greatly in the vertical direction. At low Reynolds numbers, the oscillation in the temperature values is higher than at higher Reynolds numbers. The intensity of the oscillations decreases with the increase of the Reynolds number. At W/B=0, the intensity of the oscillations increases due to the fact that the back track region of the obstacles is high. With the decrease of the back track region height, in other words when the gap ratio between the bodies increases, the oscillations decrease. The bodies act as separate bodies as long as the distance between them increases. Likewise, the interaction between the bodies gets lower and lower with the increasing gap ratio. Especially at W/B=1 and Re=10,000, there is almost no interaction between the bodies and the downstream body behaves as a single body.

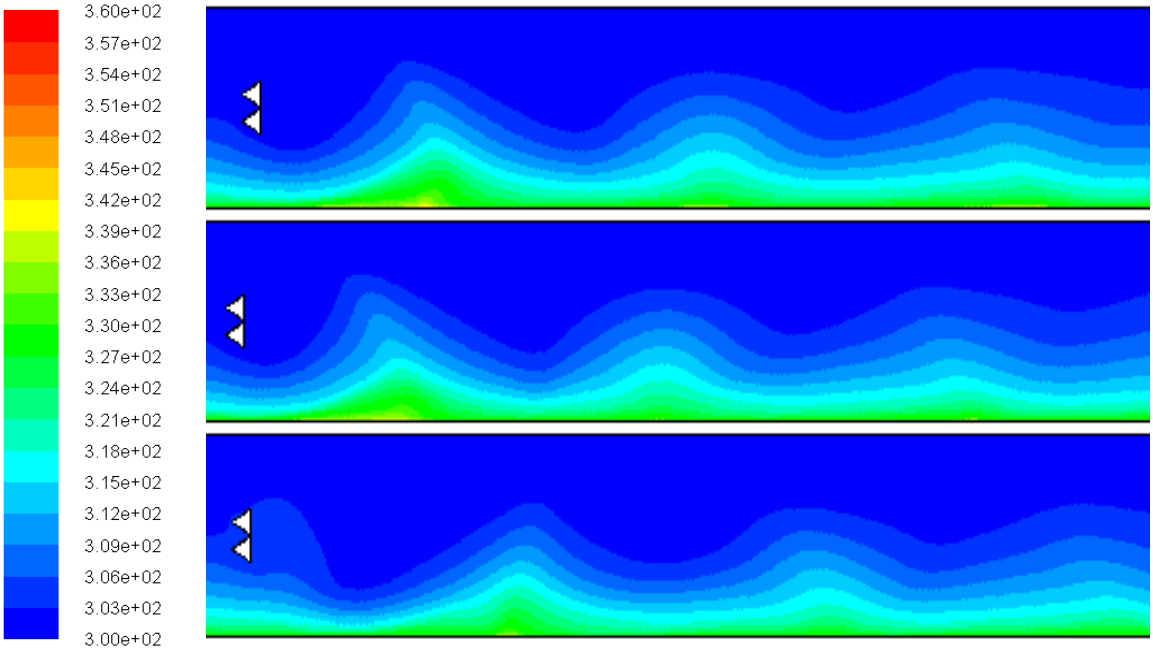

Figure 2. Temperature contours at W/B=0, Re=5000 (on the top), Re=7500 (in the middle), Re=10,000 (below).

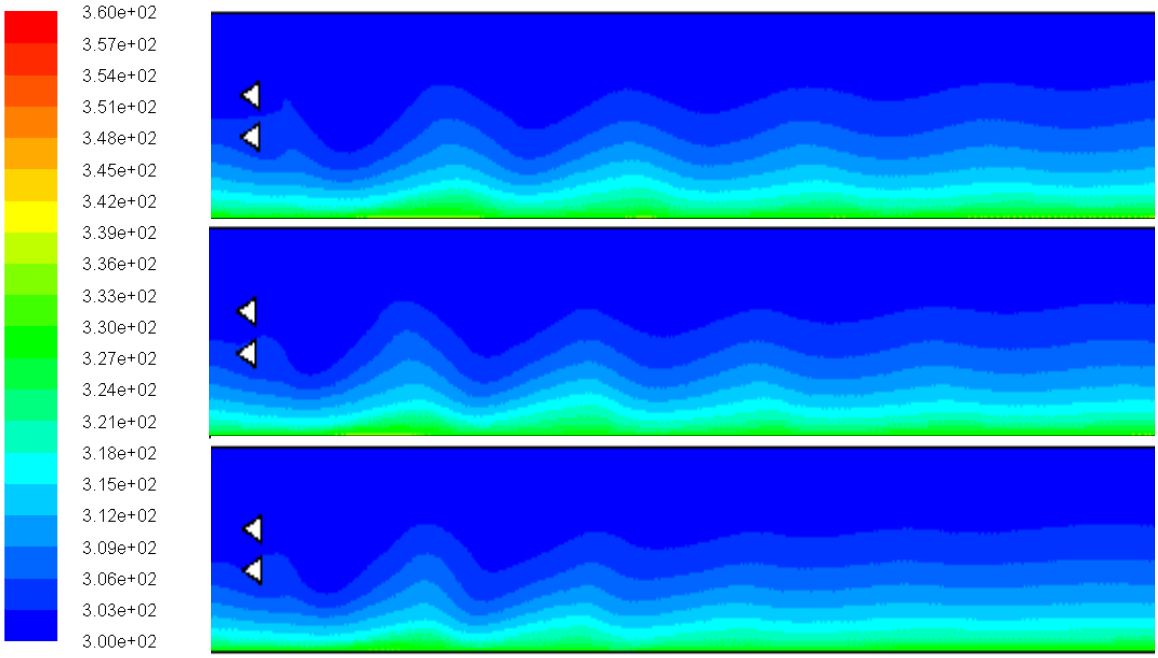

Figure 3. Temperature contours at W/B=0.5, Re=5000 (on the top), Re=7500 (in the middle), Re=10,000 (below).

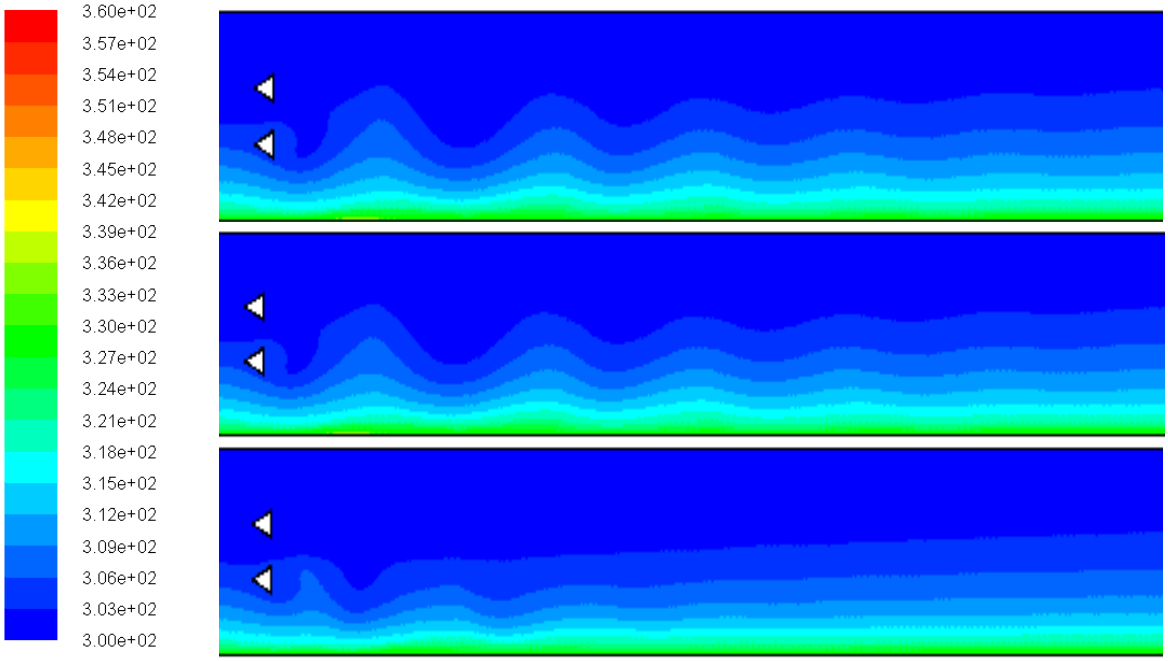

Figure 4. Temperature contours at W/B=1, Re=5000 (on the top), Re=7500 (in the middle), Re=10,000 (below).

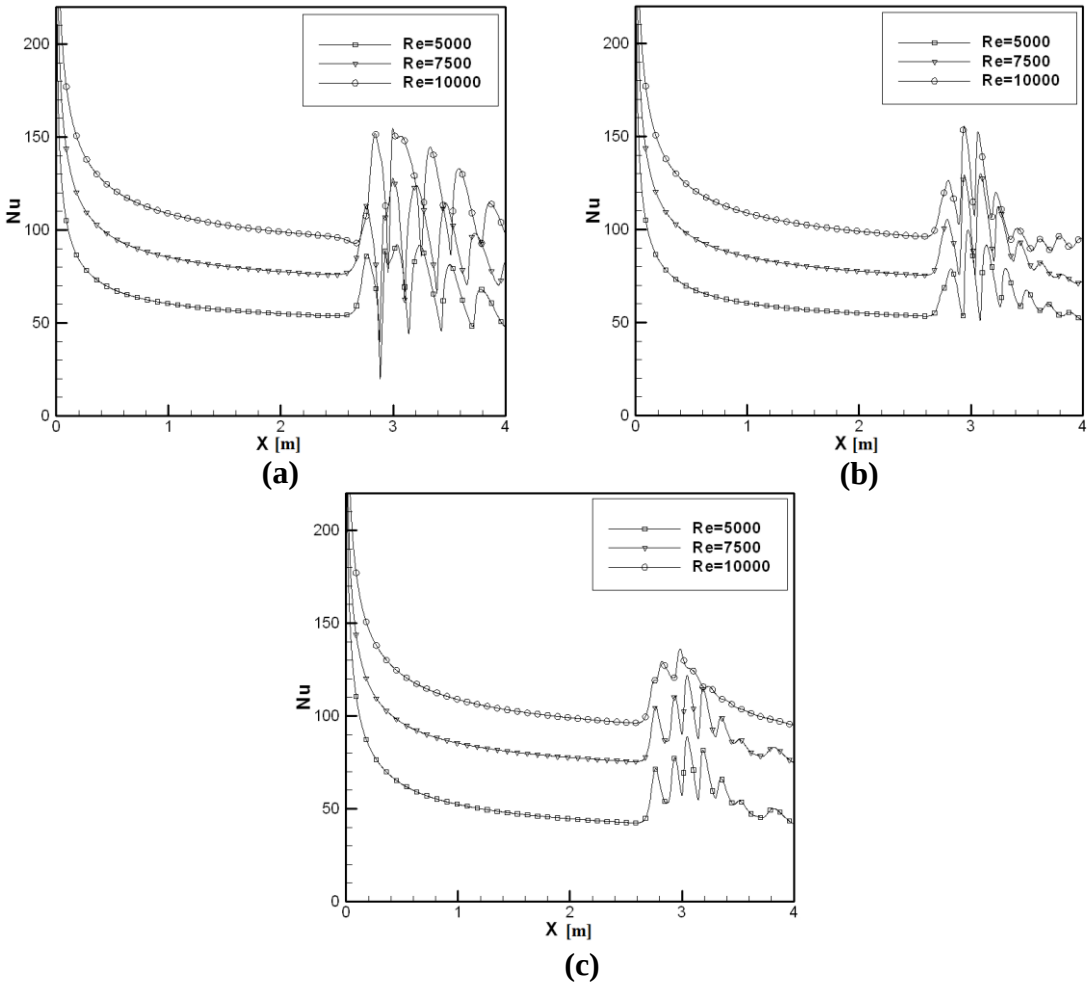

Figure 5. Local Nusselt number variations for (a) W/B=0, (b) W/B=0.5 and (c) W/B=1.

The Nusselt number variations along the bottom wall of the channel are presented in Figure 5. As the Nusselt number is a dimensionless number representing directly the heat transfer, the positions of the triangular obstacles in the channel and the Reynolds number are the important parameters in terms of the heat transfer. In all the arrangements, the Nusselt number increases after the first meeting with the bodies. At the tip of the triangles, the Nusselt number reaches a peak. Then from the tips of the triangles, the Nusselt number does not decrease, but goes on oscillating due to the flow structure and the disturbance of the viscous sublayer. The interaction and thus the blockage ratio between the bodies is an important parameter in terms of the heat transfer. At zero gap ratio (W/B=0), the highest heat transfer is provided due to the strong flow interaction. This is because the back track region of the triangles is high (2B=40 mm) and this causes the flow to oscillate. The strong fluctuations in the flow field disturb the viscous sublayer, and this causes the heat transfer to increase. With the increase of the gap ratio, the rate of increase of the Nusselt number decreases. The lowest Nusselt number value is obtained at W/B=1. As for the Reynolds number, the increase in the flow velocity enhances the heat transfer.

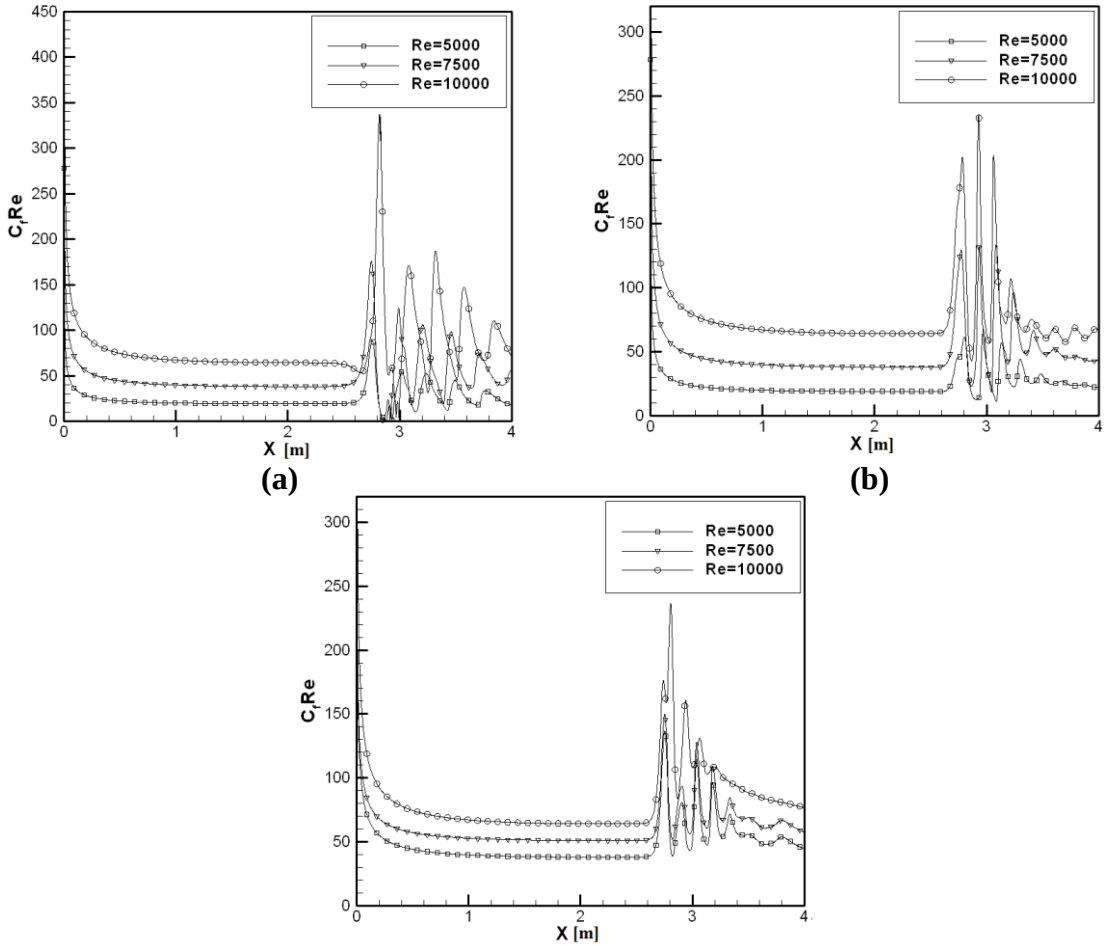

Figure 6. Local surface friction coefficient variations for (a) W/B=0, (b) W/B=0.5 and (c) W/B=1.

In the basic mean, the fact that the heat transfer provided by the insertion of the triangular elements into the channel is investigated is a heat transfer enhancement process by passive methods. An undesirable situation is the increase of the friction and thus the pumping power. The extra pumping power means extra energy consumption. In Fig. 6, the surface friction coefficient variations versus x-distance are given. Beyond the triangle tips, the friction coefficient oscillates and decreases by being damped. Towards the end of the channel, the friction coefficient goes on decreasing. The average Nusselt number variations versus Reynolds number are shown in Figure 7. It is known that the Nusselt number increases with increasing Reynolds number. Likewise, the Nusselt number increases as long as the gap ratio increases. The highest value of the Nusselt number is obtained at W/B=0 and Re=10,000, while the lowest value is obtained at W/B=1 and Re=5000. The average surface friction coefficient variations are given in Figure 8. With the increase of the Reynolds number, the surface friction factor decreases. The increase in the gap ratio causes the surface friction coefficient to decrease.

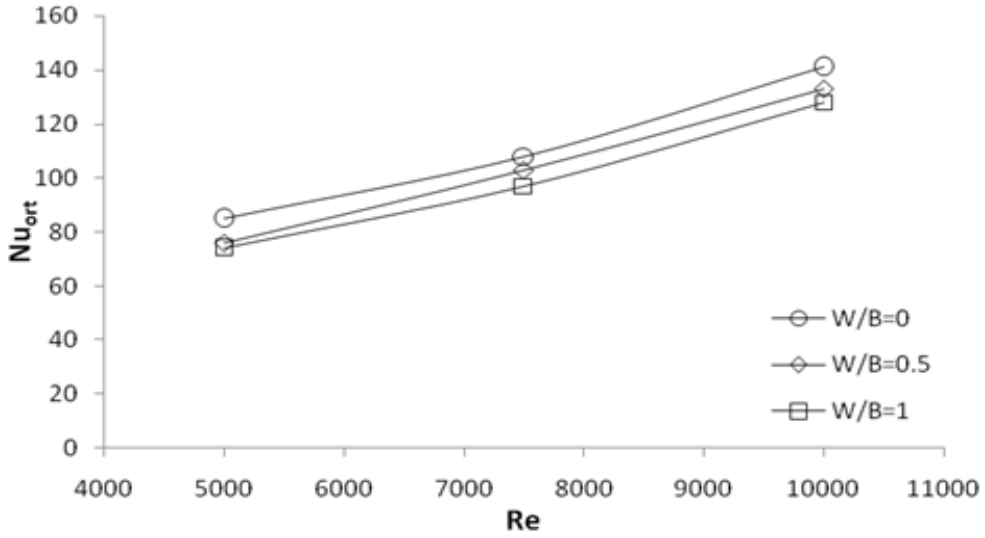

Figure 7. Average Nusselt number variations versus Reynolds number.

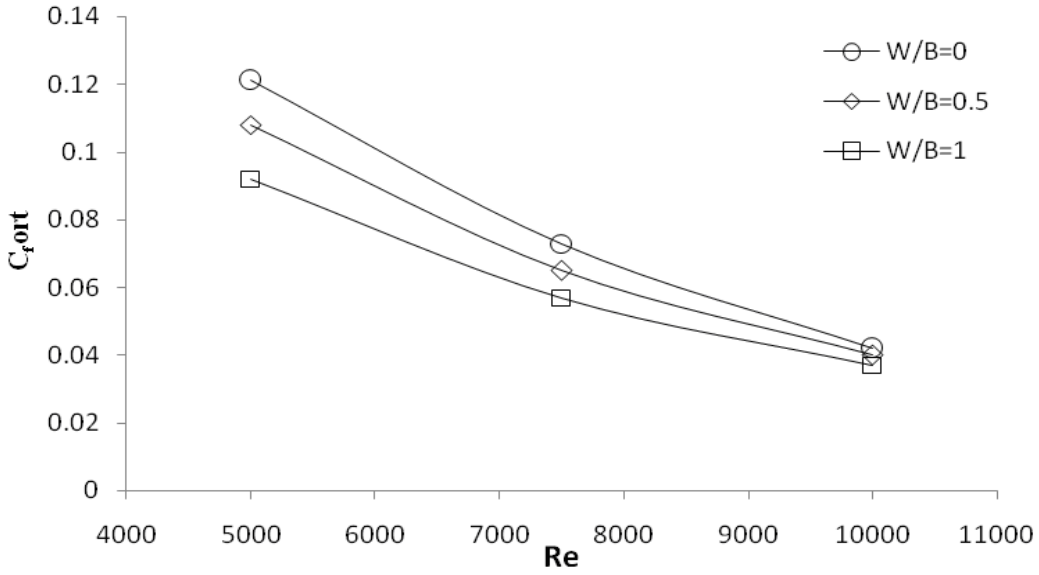

Figure 8. Average surface friction coefficient versus Reynolds number.

The overall heat transfer enhancement is presented in Figure 9 for all investigated cases. The graphs consist of two parts. Values above 1 mean there is a net energy gain and overall heat transfer enhancement. Values lower than 1 mean that no heat transfer enhancement is provided. In order to calculate the overall heat transfer enhancement, the Nusselt number and the surface friction factor values of the smooth channel must be known. In this study, the smooth channel values of both the Nusselt number and the surface friction factor have been calculated at the same flow conditions and with no triangles. For all the studied cases the overall heat transfer enhancement is provided. The overall heat transfer enhancement (OHTE) decreases with the increase of the Reynolds number. The increasing gap ratio causes the OHTE to decrease. The highest value of the OHTE is obtained with W/B=0 and Re=5000. The lowest OHTE is obtained at W/B=1 and Re=10,000.

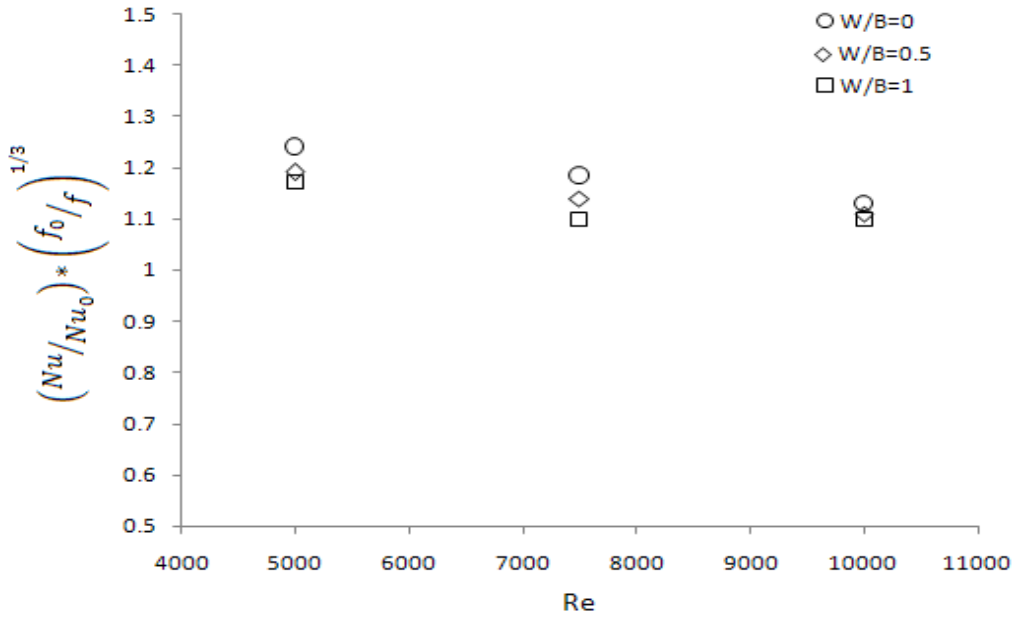

Figure 9. Overall heat transfer enhancement ratios.

CONCLUSIONS

In this numerical work, the investigation of the effects of equilateral triangular bodies on heat transfer and flow characteristics was made based on the Nusselt number and skin friction factor calculated numerically. Some significant results of this research concluded from the whole study can be summarized as follows:

Along the x distance beyond the bluff bodies, the temperature variations changed greatly in the vertical direction. The intensity of the oscillations decreased with the increase of the Reynolds number. With the decrease of the back track region height, in other words, as the gap ratio between the bodies increased, the oscillations decreased. The bodies acted as separate bodies as long as the distance between them increased. In all the arrangements, the Nusselt number increased after the first meeting with the bodies. At the tip of the triangles, the Nusselt number reached a peak. Then from the tips of the triangles, the Nusselt number did not decrease but went on oscillating due to the flow structure and the disturbance of the viscous sublayer.

The strong fluctuations in the flow field disturbed the viscous sublayer, and this caused the heat transfer to increase. With the increase of the gap ratio, the rate of increase of the Nusselt number decreased. For all the studied cases an overall heat transfer enhancement was provided. The increasing gap ratio caused the overall heat transfer enhancement (OHTE) to decrease. The highest value of the OHTE was obtained in the case of W/B=0 and Re=5000. The lowest OHTE was obtained at W/B=1 and Re=10,000.

ACKNOWLEDGMENTS

The authors would like to thank the TUBITAK (The Scientific and Technological Research Council of Turkey) for financial support under contract: 107M508.

REFERENCES

Abbassi, H., Turki, S., & Nasrallah, S. B. (2001). Numerical ınvestigation of forced convection in a plane channel with a built-in triangular prism. *International Journal of Thermal Sciences, 40,* 649-658.

Bharti, R. P., Chhabra, R. P., & Eswaran, V. (2007). Steady forced convection heat transfer from a heated circular cylinder to power-law fluids. *International Journal of Heat and Mass Transfer, 50,* 977-990.

Bhattacharyya, S. & Singh, A. K. (2010). Vortex shedding and heat transfer dependence on effective Reynolds number for mixed convection around a cylinder in cross flow. *International Journal of Heat and Mass Transfer, 53,* 3202-3212.

Chatterjee, D., Biswas, G., & Amiroudine, S. (2009). Numerical investigation of forced convection heat transfer in unsteady flow past a row of square cylinders. *International Journal of Heat and Fluid Flow, 30,* 1114-1128.

Dhiman, A. & Hasan, M. (2013). Flow and heat transfer over a trapezoidal cylinder: steady and unsteady regimes. *Asia-Pacific Journal of Chemical Engineering, 8,* 433-446.

Dhinakaran, S. (2011). Heat transport from a bluff body near a moving wall at Re = 100. *International Journal of Heat and Mass Transfer, 54,* 5444-5458.

FLUENT 6.1.22. (2001). *User's Guide*. Lebanon, NH, USA: Fluent Incorporated.

Hanafi, A. S., El-Sayed, S. A., & Mostafa, M. E. (2002). Fluid flow and heat transfer around circular cylinder – flat and curved plates combinations. *Experimental Thermal and Fluid Science, 25,* 631-649.

Hemida, H., Spehr, F., & Krajnovic, S. (2008). Local heat transfer enhancement around a matrix of wall-mounted cubes using passive flow control: large-eddy simulations. *International Journal of Heat and Fluid Flow, 29,* 1258-1267.

Igarashi, T. & Mayumi, Y. (2001). Fluid flow and heat transfer around a rectangular cylinder with small inclined angle. *International Journal of Heat and Fluid Flow, 22,* 279-286.

Juncu, G. (2007). A numerical study of momentum and forced convection heat transfer around two tandem circular cylinders at low Reynolds numbers. Part II: Forced convection heat transfer. *International Journal of Heat and Mass Transfer, 50,* 3799-3808.

Mahir, N. & Altaç, Z. (2008). Numerical investigation of convective heat transfer in unsteady flow past two cylinders in tandem arrangements. *International Journal of Heat and Fluid Flow, 29,* 1309-1318.

Manay, E. (2010). *Experimental and numerical investigation of heat transfer and flow characteristics in a channel equipped with triangular inner elements* (MS Thesis). Erciyes University.

Meinders, E. R. & Hanjalic, K. (2002). Experimental study of the convective heat transfer from in-line and staggered configurations of two wall-mounted cubes. *International Journal of Heat and Mass Transfer, 45,* 465-482.

Nakamura, H., Igarashi, T., & Tsutsui, T. (2003). Local heat transfer around a wall-mounted cube at 45^{o} to flow in a turbulent boundary layer. *International Journal of Heat and Fluid Flow, 24,* 807-815.

Rosales, J. L., Ortega, A., & Humphrey, J. A. C. (2001). A numerical simulation of the convective heat transfer in confined channel flow past square cylinders:

Comparison of inline and offset tandem pairs. *International Journal of Heat and Mass Transfer, 44*, 587-603.

Srikanth, S., Dhiman, A. K., & Bijjam, S. (2010). Confined flow and heat transfer across a triangular cylinder in a channel. *International Journal of Thermal Sciences, 49*, 2191-2200.

Sripattanapipat, S. & Promvonge, P. (2009). Numerical analysis of laminar heat transfer in a channel with diamond-shaped baffles. *International Communications in Heat and Mass Transfer, 36*, 32-38.

Sumner, D. (2010). Two circular cylinders in cross-flow: A review. *Journal of Fluids and Structures, 26*, 849-899.

Tahseen, T. A., Ishak, M., & Rahman, M. M. (2012). A numerical study of forced convection heat transfer over a series of flat tubes between parallel plates. *Journal of Mechanical Engineering and Sciences*, 3, 271-280.

Velayati, E. & Yaghoubi, M. (2005). Numerical study of convective heat transfer from an array of parallel bluff plates. *International Journal of Heat and Fluid Flow, 26*, 80-91.

Wang, L. Salewski, M., Sundén, B., Borg, A., & Abrahamsson, H. (2012). Endwall convective heat transfer for bluff bodies. *International Communications in Heat and Mass Transfer, 39*, 167-173.